

Brillouin microscopy, what is it really measuring?

Pei-Jung Wu^{1,2}, Irina Kabakova², Jeffrey Ruberti³, Joseph M. Sherwood¹, Iain E. Dunlop⁴,
Carl Paterson², Peter Török^{2*}, Darryl R. Overby^{1*}

¹ Imperial College London, Department of Bioengineering, London UK

² Imperial College London, Department of Physics, London UK

³ Northeastern University, Department of Bioengineering, Boston, MA USA

⁴ Imperial College London, Department of Materials, London UK

*co-corresponding authors

Abstract

Brillouin microscopy is a new tool to characterize the stiffness of cells and tissues, however the underlying relationship between stiffness and Brillouin measurements remains unknown. As the stiffness of biological materials is influenced by hydration, we performed Brillouin microscopy on hydrogels whilst independently examining the role of stiffness and water content. Brillouin measurements were independent of stiffness, but correlated strongly with hydration, indicating that Brillouin microscopy really measures water content.

Main Text

Brillouin microscopy is a non-invasive label-free method to map the micromechanical properties of cells and tissues with high spatial resolution^{1,2}. Brillouin microscopy is gaining attention as a promising form of optical micro-elastography³, with a growing number of applications in cardiovascular disease⁴, ophthalmology⁵⁻⁷, and cellular mechanics^{2,8-10}.

Based on the phenomenon of Brillouin scattering, photons exchange energy with thermally-driven acoustic waves, or phonons, leading to a frequency shift between incident and scattered light. This frequency shift, ω_b , is measured by Brillouin microscopy and given by

$$\omega_b = \frac{2n}{\lambda} \sqrt{\frac{M}{\rho}} \sin \frac{\theta}{2} \quad \text{Eq. 1}$$

where ρ and n are the density and refractive index of the material, and λ and θ are the *in vacuo* wavelength and angle between incident and scattered wave vectors. M is the longitudinal modulus that describes the mechanical stress necessary to impose a volume change in the material by compressing or expanding it in one direction.

Biological materials are composed largely of water, which is relatively incompressible. M is therefore on the scale of 10^9 Pa, which is many orders of magnitude larger than the Young's modulus, E , for cells and tissues that ranges from 10^2 – 10^6 Pa. The Young's modulus describes the stress necessary to compress or extend a material in one direction without imposing a volume change, and represents the stiffness of a material, i.e. how resistive it is to deformation. Despite the different magnitudes of M and E , empirical correlations between these two moduli for cells², hydrogels^{2,8} and other biological tissues⁶ have given the impression that variations in M , as measured by Brillouin microscopy, reflect variations in E . Hence, Brillouin micrographs have been presented as *de facto* "stiffness maps" that could purportedly be used to assess spatial or temporal variations in the Young's modulus^{2,4,9}.

Motivated by these studies and the potential for Brillouin microscopy as a revolutionary tool for micro-elastography, we set out to more closely examine the relationship between

Brillouin microscopy and Young's modulus using hydrogels. We chose hydrogels as a model for biological materials because they both contain water interspersed within a flexible network that provides elasticity.

The Young's modulus of polyethylene oxide (PEO) hydrogels depends on both molecular weight and water content, ε .¹¹ By varying the molecular weight for three different values of water content, we independently investigated the effects of E and ε (Figure 1A), and measured the longitudinal or "Brillouin modulus" M . While E increased with molecular weight, there was no apparent increase in M for any given value of ε (Figure 1B). Hence, between PEO hydrogels of differing Young's moduli, there was no detectable change in the Brillouin modulus. In contrast, a single relationship between M and ε completely characterized all samples (Figure 1C), with $R^2=0.97$, indicating that 97% of the variance in Brillouin modulus could be attributed to the variance in water content.

Previous correlations between M and E were reported based on polyacrylamide (PA) hydrogels^{2,8}. PA hydrogels swell, and thereby increase their water content over time (Figure 2A). We used six different cross-linker concentrations to vary stiffness, and measured the Brillouin modulus, Young's modulus and the water content during swelling to investigate the relationships between M , E and ε for individual hydrogels.

During swelling, the Brillouin modulus decreased significantly, while the Young's modulus remained nearly constant or decreased only slightly (Figure 2B). Brillouin data from all time points collapsed onto a single curve when M was plotted versus ε (Figure 2C), with $R^2=0.92$. Hence, changes in M for individual PA hydrogels were not directly related to changes in E , but were tightly correlated with changes in ε .

These data reveal, using two chemically distinct hydrogels, that there is no simple one-to-one relationship between Young's modulus and Brillouin modulus for hydrated materials, even within a given sample. In contrast, over a wide range of Young's moduli and swelling times, Brillouin modulus could be described almost entirely by a dependence on ε .

As cells and tissues, like hydrogels, are composed largely of water, we would expect that Brillouin microscopy would be equally sensitive to water content when applied to biological materials. This work cautions against the straightforward use of Brillouin microscopy, or Brillouin scattering in general, as a form of optical elastography, but suggests that Brillouin microscopy may be well suited for investigating mechanisms involving local hydration, such as cell volume regulation, intracellular phase changes and polymerization.

Methods

Methods are given in the supplemental information.

References

1. Scarcelli, G. & Yun, S. H. *Nat. Photonics* **2**, 39–43 (2008).
2. Scarcelli, G. *et al.* *Nat. Methods* **12**, 1132–1134 (2015).
3. Kennedy, B. F., Wijesinghe, P. & Sampson, D. D. *Nat. Photonics* **11**, 215–221 (2017).
4. Antonacci, G. *et al.* *J R Soc. Interface* **12**, 20150843 (2015).
5. Scarcelli, G., Besner, S., Pineda, R., Kalout, P. & Yun, S. H. *JAMA Ophthalmol.* **133**, 480–482 (2015).
6. Scarcelli, G., Kim, P. & Yun, S. H. *Biophys. J.* **101**, 1539–1545 (2011).
7. Lepert, G., Gouveia, R. M., Connon, C. J. & Paterson, C. *Faraday Discuss.* **187**, 415–428 (2016).
8. Antonacci, G. & Braakman, S. *Sci. Rep.* **6**, 37217 (2016).
9. Zhang, J., Nou, X. A., Kim, H. & Scarcelli, G. *Lab Chip* **17**, 663–670 (2017).
10. Meng, Z., Petrov, G. I., & Yakovlev, V. V. *Analyst* **140**, 7160–7164 (2015).
11. de Gennes, P. G. *Scaling Concepts in Polymer Physics* (Cornell Univ. Press, 1979).

Figures

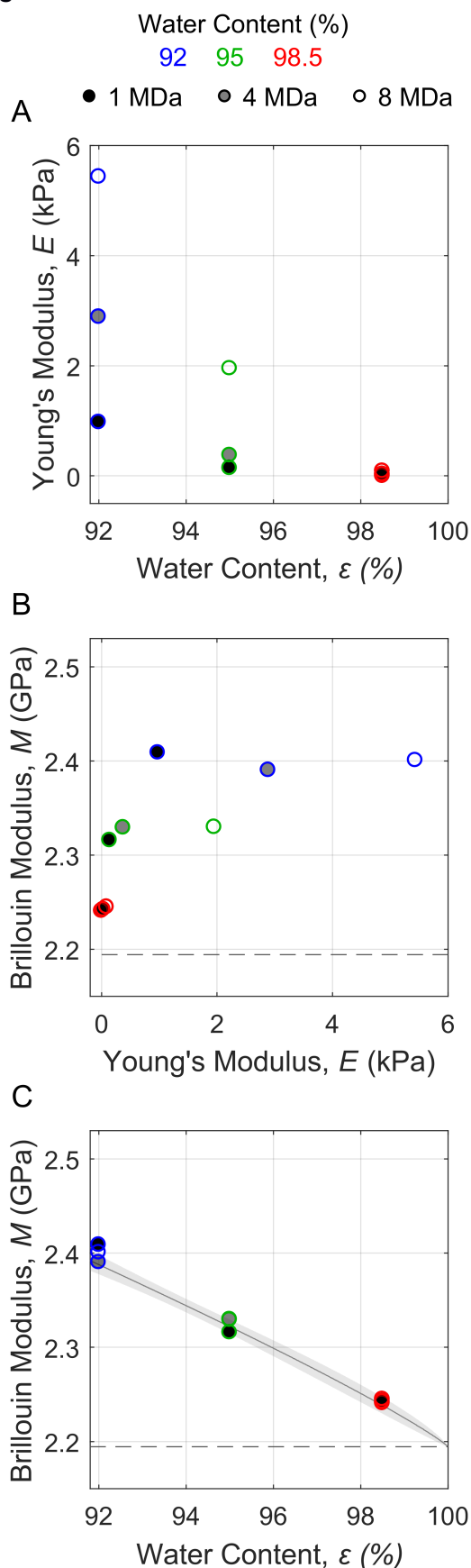


Figure 1: Polyethylene oxide hydrogels of varying molecular weight were used to examine independently the effect of Young's modulus E and water content ϵ on the longitudinal modulus measured by Brillouin microscopy M . (A) With increasing molecular weight, E increased for a given value of ϵ due to increasing entanglements between longer polymer chains. (B) For a given water content, increasing the Young's modulus did not coincide with a change in the Brillouin modulus. (C) However, data for all values of M collapsed onto a single curve when plotted versus ϵ ($R^2 = 0.97$). Colors represent water content, with shading within the symbols representing molecular weight. Dashed horizontal lines in panels B and C represent the longitudinal modulus of pure water. Data in panel C were fit by a power-law relationship of the form $M - M_w = \alpha(1 - \epsilon)^\beta$, with shaded regions representing the 95% confidence bounds on the fit. Data points correspond to individual hydrogels.

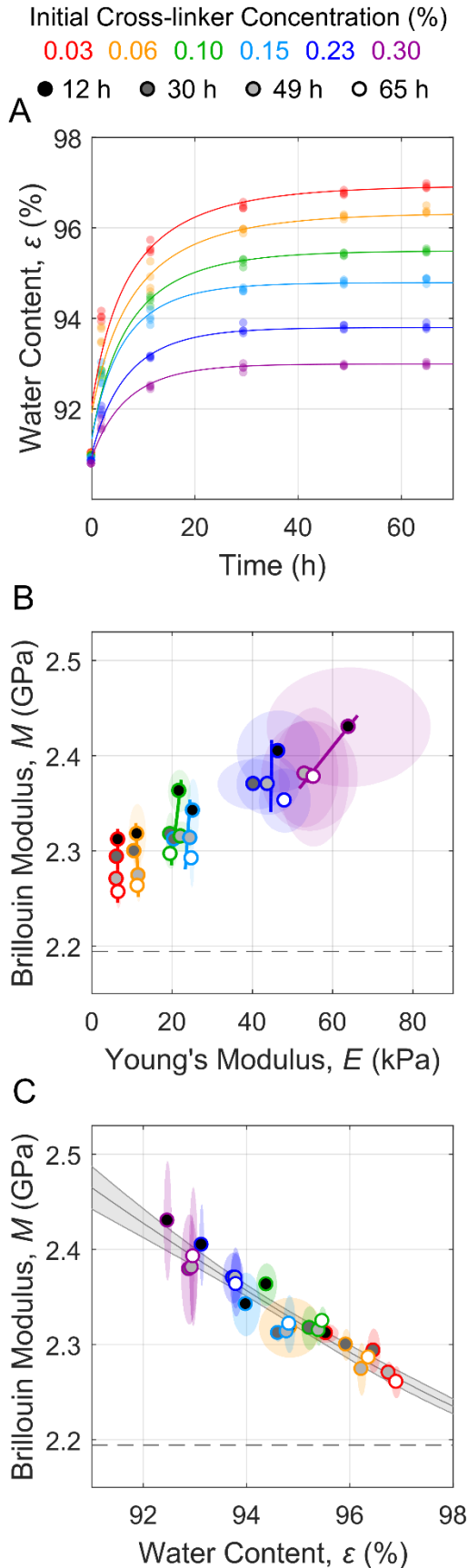


Figure 2: Polyacrylamide hydrogels of varying bis-acrylamide cross-linker concentration were allowed to swell in water, whilst we measured the water content ε , Young's modulus E , and longitudinal modulus with Brillouin microscopy M . (A) Water content ε increased over time due to swelling, with greater swelling observed for lower cross-linker concentrations. Curves show exponential fits. (B) During swelling, the Brillouin modulus decreased while the Young's modulus remained the same or decreased only slightly. Lines show the best fit of how M changes versus E over time. (C) Brillouin data from all time points collapsed onto a single curve when plotted versus ε ($R^2=0.92$). Colors represent different cross-linker concentrations. Dashed horizontal lines in panels B and C represent the longitudinal modulus of pure water. Data in (C) were fit by a power-law relationship of the form $M - M_w = a(1 - \varepsilon)^\beta$, with shaded regions representing the 95% confidence bounds on the fit. Elliptical regions surrounding the data points represent the two standard deviations on each measurement ($n = 4$).

Supplemental Methods

1. Hydrogel Preparation

1.1 Polyacrylamide (PA)

PA hydrogels were prepared following a published protocol.¹ Hydrogel stiffness was adjusted by varying the ratio of acrylamide, bis-acrylamide and distilled water. For all samples, the initial concentration of acrylamide (Sigma-Aldrich) was 10% (w/v). N-methylene-bis-acrylamide (Sigma-Aldrich) was added at an initial concentration of 0.03, 0.06, 0.10, 0.15, 0.23, and 0.30% (w/v). The mixtures were centrifuged at 500g for 5 minutes, followed by the addition of 0.1% (w/v) ammonium persulfate (Sigma-Aldrich) and 0.1% tetramethylethylenediamine (Sigma-Aldrich) to initiate polymerization. The mixture was cast into disk-shaped molds (diameter 20 mm, depth 5 mm) and allowed to polymerize for 15 minutes. The hydrogels were then removed and immersed fully in a large container of distilled water to swell freely. Data shown in the main text were from a single experiment with 4 replicate hydrogels made from the same stock solution for each cross-linker concentration. Hydrogel mass was measured for each replicate immediately after polymerization and at 2, 12, 30, 49, and 65 hours using an electronic balance with a precision of 1 mg (see Fig. S1A). Brillouin microscopy, compression tests and refractometry were performed for each replicate at 12, 30, 49, and 65 hours after polymerization.

The water content, ε , of PA hydrogels increased during swelling, and was calculated according to:

$$\varepsilon(t) = \frac{\text{volume of water}}{\text{volume of hydrogel}} = \frac{V_{w,0} + \Delta V_w(t)}{V_0 + \Delta V_w(t)} \quad (\text{S1})$$

where V_0 is the initial hydrogel volume determined by the volume of the mold, $V_{w,0}$ is the volume of water in the hydrogel at the start of polymerization, and $\Delta V_w(t)$ is the volume of water imbibed during swelling. $V_{w,0}$ was calculated according to

$$V_{w,0} = V_0 - \frac{M_a}{\rho_a} - \frac{M_b}{\rho_b} \quad (\text{S2})$$

where M_a , ρ_a and M_b , ρ_b are the mass and density of acrylamide ($\rho_a = 1.13 \text{ g/cm}^3$) and bis-acrylamide ($\rho_b = 1.235 \text{ g/cm}^3$), respectively. $\Delta V_w(t)$ was calculated according to

$$\Delta V_w(t) = \frac{M(t) - M_0}{\rho_w} \quad (\text{S3})$$

where ρ_w is the density of water ($\rho_w = 1.00 \text{ g/cm}^3$), $M(t)$ is the hydrogel mass at time t , and M_0 is the hydrogel mass immediately after polymerization. The density of the hydrogel decreased during swelling (Fig. S1B), and was calculated according to:

$$\rho(t) = \frac{\text{mass of hydrogel}}{\text{volume of hydrogel}} = \frac{M(t)}{V_0 + \Delta V_w(t)} \quad (\text{S4})$$

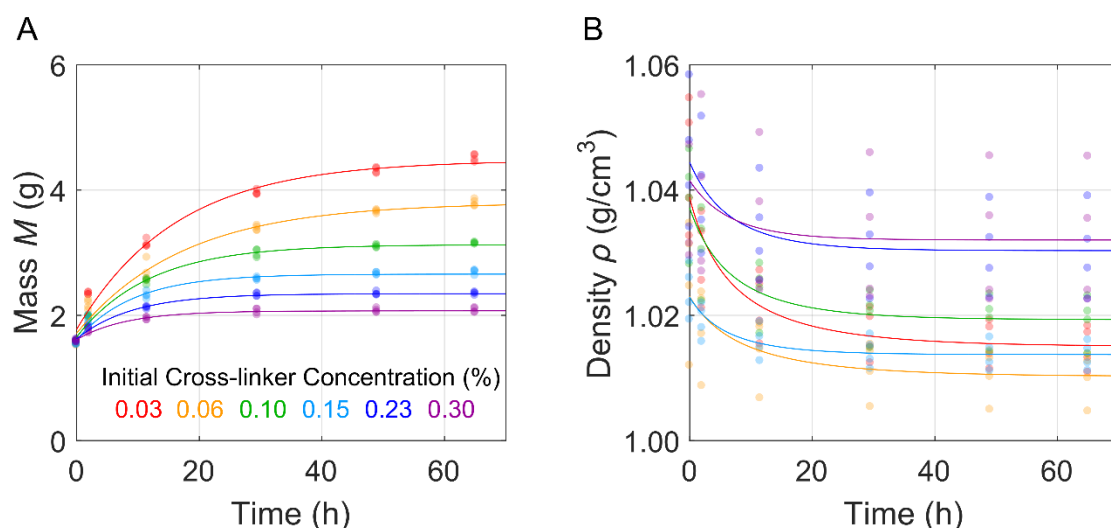


Figure S1: Polyacrylamide hydrogels of varying initial bis-acrylamide concentration during swelling. (A) Hydrogel mass increased during swelling, with larger swelling observed for lower initial cross-linker concentrations. (B) Density decreased during swelling, as calculated by Eq. S4. Each data point is an individual replicate ($n = 4$) made from the same stock solution. Curves show best exponential fits.

1.2 Polyethylene oxide (PEO)

PEO hydrogels were made with an average molecular weight of 1, 4, and 8 MDa (Sigma-Aldrich). Mixtures of 1.5%, 5.0%, and 8.0% (w/v) PEO (corresponding to $\varepsilon = 0.985, 0.95$ and 0.92 , respectively) were prepared in distilled water with continuous magnetic stirring at 1000 rpm for at least 10 hours until the mixture was homogeneous. Data shown in the main text were from a single experiment with one hydrogel for each water content and molecular weight. A single sample volume was taken to measure refractive index for each condition. A further single sample volume was taken for Brillouin microscopy for each condition. For rheometry, 2-3 sample volumes were measured for each condition. PEO hydrogels were not allowed to swell and were mixed and stored in a sealed container to minimize evaporation. Density for the PEO hydrogels was calculated according to:

$$\rho = \frac{M_w + M_p}{V_w + V_p} = \frac{M_w + M_p}{\frac{M_w}{\rho_w} + \frac{M_p}{\rho_p}} \quad (\text{S5})$$

where M_w , ρ_w , M_p and ρ_p are the mass and density of added water and polymer ($\rho_p = 1.21$ g/cm³), respectively.

2. Brillouin microscopy

2.1 Experimental setup

Figure S2A shows the optical setup for Brillouin microscopy, following previous studies². An objective lens (20X, NA = 0.5, Olympus) focused the light of a single longitudinal mode cobalt laser ($\lambda=561$ nm; 30 mW, Cobolt Jive) emerging from single-mode optical fiber (Kineflex, OptiQ). Thus, an approximately 7 μm^3 volume of the sample was illuminated. Backscattered light from this volume was collected by the same objective and coupled into a single-mode

optical fiber delivering the light to a custom-built spectrometer, consisting of an interferometer², a virtually imaged phased array (VIPA) and a Neo sCMOS camera (Andor). The interferometer suppresses the Rayleigh peaks before the signal passes through the VIPA (FSR = 39 GHz, LightMachinery Inc.) etalon that spatially separates the frequency components. For each PA or PEO sample, three randomly-selected locations were measured throughout the hydrogel, with 50 spectra acquired at each location and averaged. The illumination and detection side single mode optical fibers together ensure that the optical system embodies a Type II confocal microscope³ which ensured that only light from the 7 μm^3 volume of the sample was collected. This was important because measurements assume sample homogeneity within this volume.

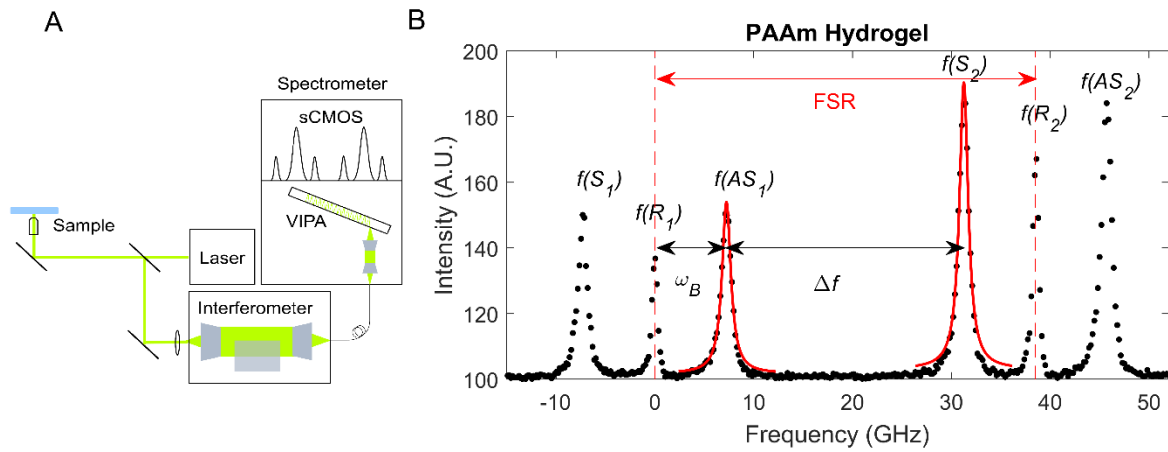


Figure S2: Acquisition and analysis of Brillouin microscopy. (A) Schematic of the Brillouin microscope. Laser light is directed into an inverted confocal microscope. Backscattered light is collected and filtered to reduce the intensity of the Rayleigh peak by up to 40dB. The filtered signal passes through a VIPA to separate spectral components that are detected by an sCMOS camera. (B) Pixels in the spectrum are converted into frequency (see details in text) to identify the Brillouin frequency shift ω_b after the peaks are fitted by a Lorentzian function, where $\omega_b = (FSR - \Delta f)/2$.

2.2 Data analysis

The Brillouin modulus M was calculated, following measurements of the Brillouin frequency shift ω_b , refractive index n , and density ρ , according to:

$$M = \rho \left(\frac{\lambda \omega_b}{2 n \sin \frac{\theta}{2}} \right)^2 \quad (\text{S6})$$

where λ and θ are the wavelength and angle between the incident and scattered wave vectors, defined to be 561 nm and $\pi/2$, respectively. Brillouin frequency shift was measured based on the frequency difference between the Rayleigh and Stokes peaks, as described below. Density was calculated according to Equations S4 or S5. Refractive index was measured using an Abbe refractometer (Bellingham and Stanley Ltd., London; Fig. S3).

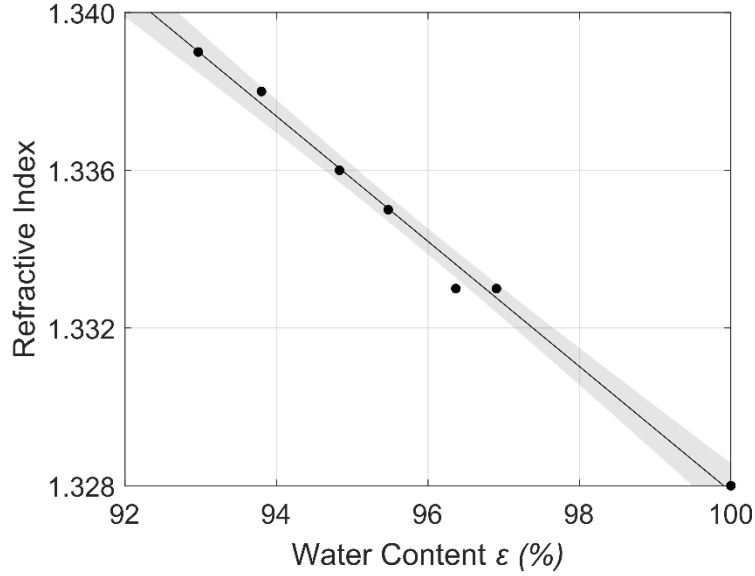


Figure S3: Refractive index of PA hydrogels measured at 65 hours decreased with increasing water content.

Raw images of spectra were calibrated to convert pixels to frequency. To do this, we identified the line connecting the Rayleigh, Stokes, and anti-Stokes Brillouin peaks of two orders. A peak finding algorithm was performed to locate the six peaks, applying moving average to reduce random noise. The positions of these peaks were then used to map pixel location x to frequency f based on known free spectral range (FSR) based on a quadratic relationship $f(x) = ax^2 + bx + c$, where parameters a , b and c are determined by minimising the least squared error of the following 8 relationships:

$$\begin{bmatrix} f(R_1) \\ f(R_2) \\ f(R_2 - R_1) \\ f(S_2 - S_1) \\ f(AS_2 - AS_1) \\ f(AS_1 - R_1) - f(R_1 - S_1) \\ f(AS_2 - R_2) - f(R_2 - S_2) \\ f(AS_2 - S_2) - f(AS_1 - S_1) \end{bmatrix} = \begin{bmatrix} 0 \\ FSR \\ FSR \\ FSR \\ FSR \\ 0 \\ 0 \\ 0 \end{bmatrix} = \begin{bmatrix} x_1^2 & x_1 & 1 \\ x_2^2 & x_2 & 1 \\ x_3^2 & x_3 & 1 \\ x_4^2 & x_4 & 1 \\ x_5^2 & x_5 & 1 \\ x_6^2 & x_6 & 1 \\ x_7^2 & x_7 & 1 \\ x_8^2 & x_8 & 1 \end{bmatrix} \begin{bmatrix} a \\ b \\ c \end{bmatrix} \quad (S6)$$

where R_n , S_n , and AS_n are the locations of the Rayleigh peak and the Stokes and anti-Stokes Brillouin peaks of the n^{th} order ($n=1$ or 2).

Lorentzian functions were independently fitted to the Stokes and anti-Stokes peaks, and the frequency difference between the peaks, Δf , was calculated (Fig. S2B). The Brillouin frequency shift ω_B is:

$$\omega_B = \frac{1}{2}(FSR - \Delta f) \quad (S7)$$

3. Measurement of Young's modulus

3.1 PA hydrogels

The instantaneous elastic modulus of PA hydrogels was measured in unconfined uniaxial compression using an Instron Model 5866 fitted with a 50 N load cell. The samples were preloaded to 0.01-0.05 N for one minute, then compressed to 5% strain at a crosshead speed of 0.5 mm/min for 2 cycles. Compression modulus was obtained from the linear fit of the second cycle in the stress-strain curve. The area was calculated based on the diameter measured using digital calipers with a precision of 0.01 mm. Measurements were done at room temperature.

3.2 PEO hydrogels

Dynamic rheological measurements were performed in a controlled shear rate rheometer (AR 2000; TA Instruments) in cone plate configuration with a 40 mm diameter and a 2 degree cone angle. The PEG hydrogels were tested at 25°C using an oscillating frequency sweep from 0.1 to 10 Hz at 1% strain. All tests were conducted in the linear viscoelastic range. Rheology Advantage software (TA Instruments) was used to obtain storage modulus G' and loss modulus G'' at 1 Hz. Under the assumption of incompressibility, the Young's modulus was then calculated according to $E = 3G'$.

4. Code Availability

The custom Matlab code to analyze the data is available from the corresponding authors on reasonable request.

5. Data Availability

The data sets generated and analyzed during the current study are available from the corresponding authors on reasonable request.

References

1. Tse, J.R. & Engler, A.J. Preparation of hydrogel substrates with tunable mechanical properties. *Current protocols in cell biology / editorial board, Juan S. Bonifacino ... [et al.] Chapter 10*, Unit 10 16 (2010).
2. Lepert, G., Gouveia, R.M., Connon, C.J. & Paterson, C. Assessing corneal biomechanics with Brillouin spectro-microscopy. *Faraday Discussions* **187**, 415-428 (2016)
3. Wilson, T & Sheppard C.J.R: [*Theory and practice of scanning optical microscopy*](#) London: Academic Press, 1984.